

Supporting Information

Interface-Engineered N-doped Carbon Dot/CdSe Nanoconjugates as Efficient Bi-functional Electrocatalyst in Alkaline Media

Rituparna Dutta^a, Gokul Sivaguru^a, Uday Kumar Ghorui^{a,b}, Aswathi Mangalasseri^a, Sabyasachi Chakraborty^{a,c,*}

^a Department of Chemistry, School of Engineering and Sciences (SEAS), SRM University - AP, Amaravati, Andhra Pradesh 522240, India.

^b Department of Chemistry, Indian Institute of Technology Gandhinagar, Palaj, Gujarat 382355, India

^c Centre for Interdisciplinary Research, SRM University - AP, Amaravati, Andhra Pradesh 522240, India.

***Corresponding Author:**

Dr. Sabyasachi Chakraborty; Email ID: sabyasachi.c@srmmap.edu.in

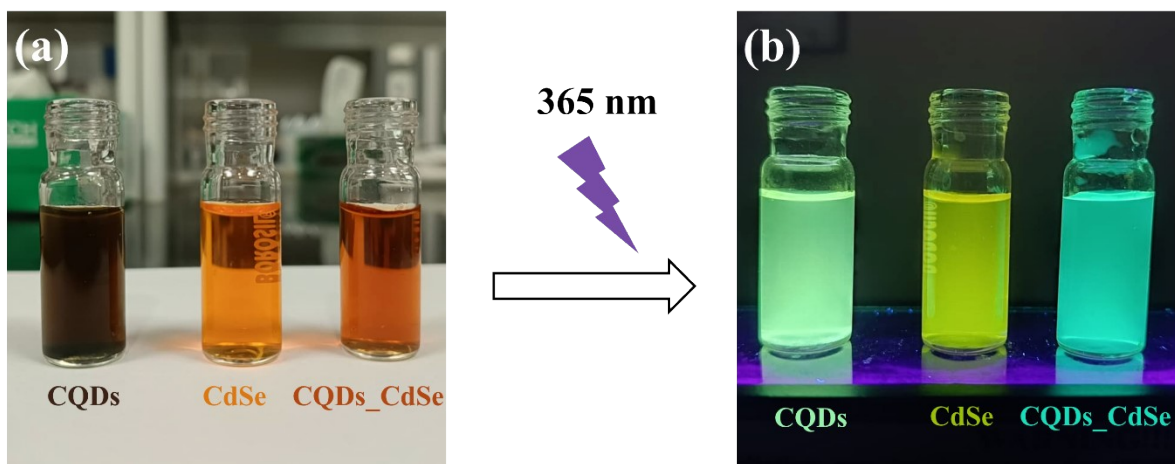


Figure S1: Digital images (A) under normal light & (B) under 365 nm UV lamp of (a) CQDs, (b) CdSe QDs, (c) CQDs_CdSe

Table S1: Calculation for average lifetime

S No	Material	τ_1 (ns)	α_1	τ_2 (ns)	α_2	τ_3 (ns)	α_3	$\langle \tau \rangle$ (ns)
1	CQDs	0.35	2.86	3.85	50.23	10.10	46.90	6.70
2	CdSe	3.18	32.92	0.23	13.23	20.30	53.85	12
3	CQDs_CdSe	3.59	32.36	10.90	62.26	0.29	5.38	7.9

Table S2: Measurement of zeta potential

Sample name	Measurement 1	Measurement 2	Measurement 3	Average ZP
CQDs	-17.1	-16.8	-18.4	-17.43 ± 0.49
CdSe	-19.7	-26.8	-27.7	-24.73 ± 2.53
CQDs_CdSe	-30.9	-32.1	-31.7	-31.56 ± 0.35

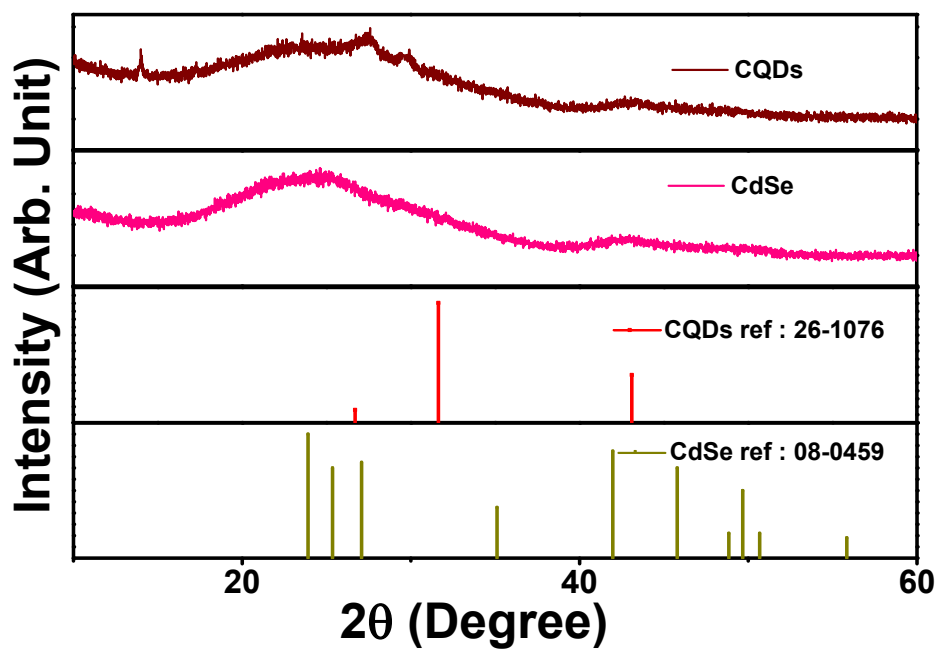


Figure S2: PXRD patterns of synthesized CQDs, CdSe QDs

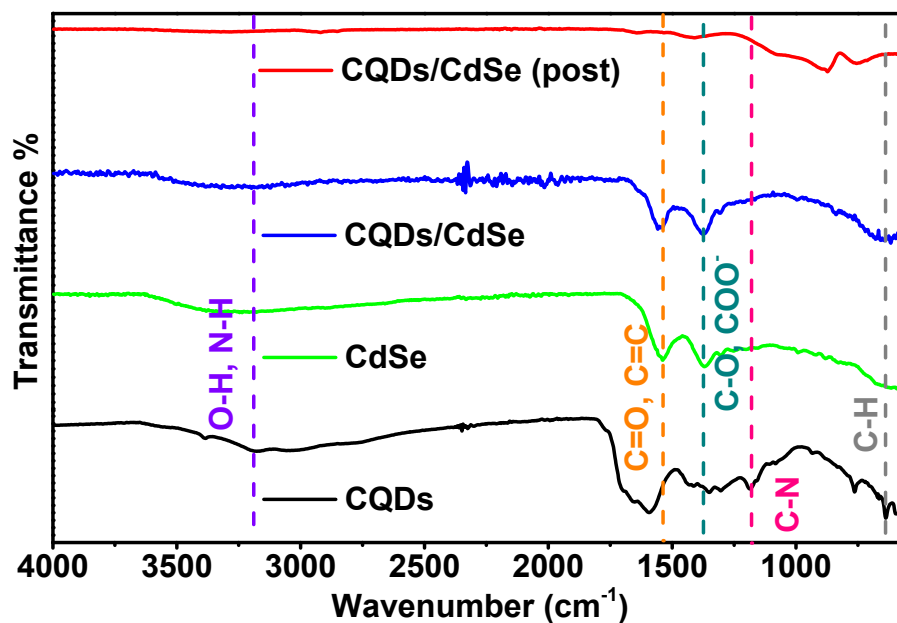


Figure S3: FTIR spectra of synthesized CQDs, CdSe QDs, CQDs/CdSe (before and after electrolysis)

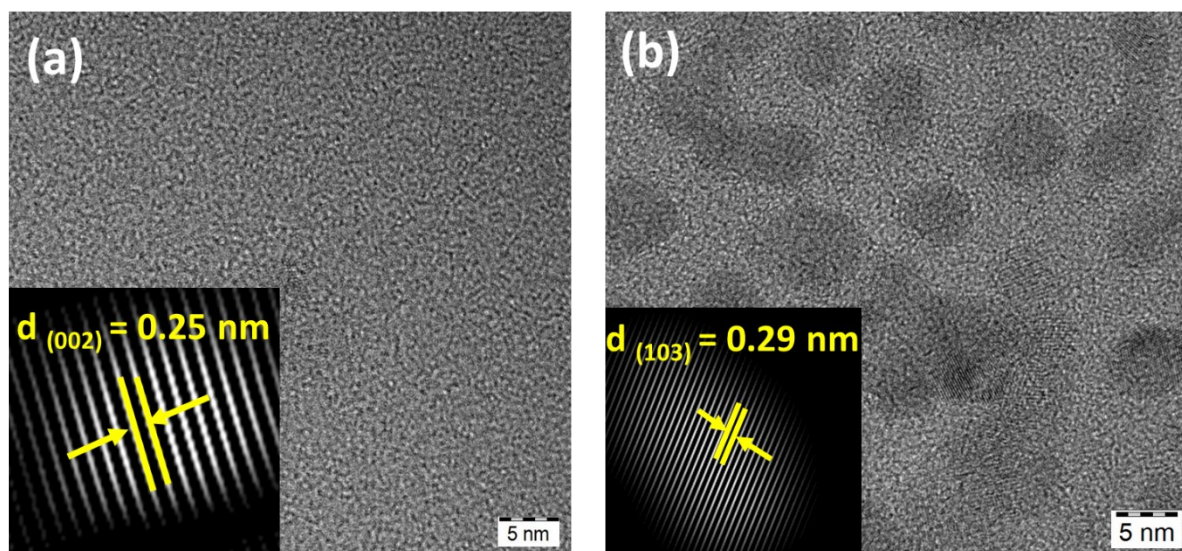


Figure S4: HRTEM image of (a) CQDs quantum dot, and (b) CdSe quantum dots with the respective inverse Fast Fourier Transform images and lattice spacing values in the inset.

Table S3: Elemental composition of CQDs/CdSe

Elements	Atomic %
Cd 3d	3.9
Se 3d	3.6
C 1s	92.5

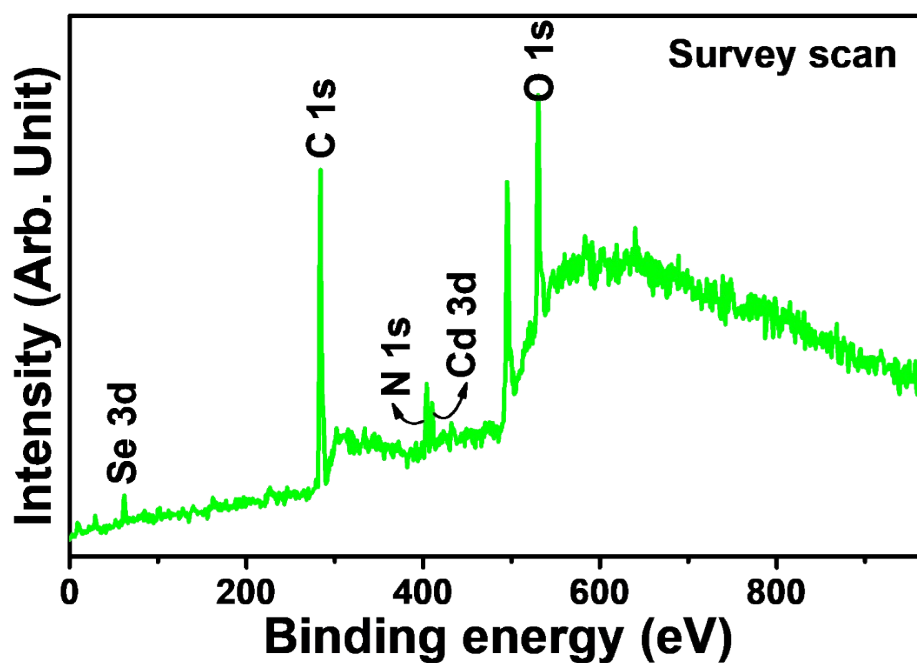


Figure S5: XPS Survey spectra of synthesized CQDs/CdSe QDs

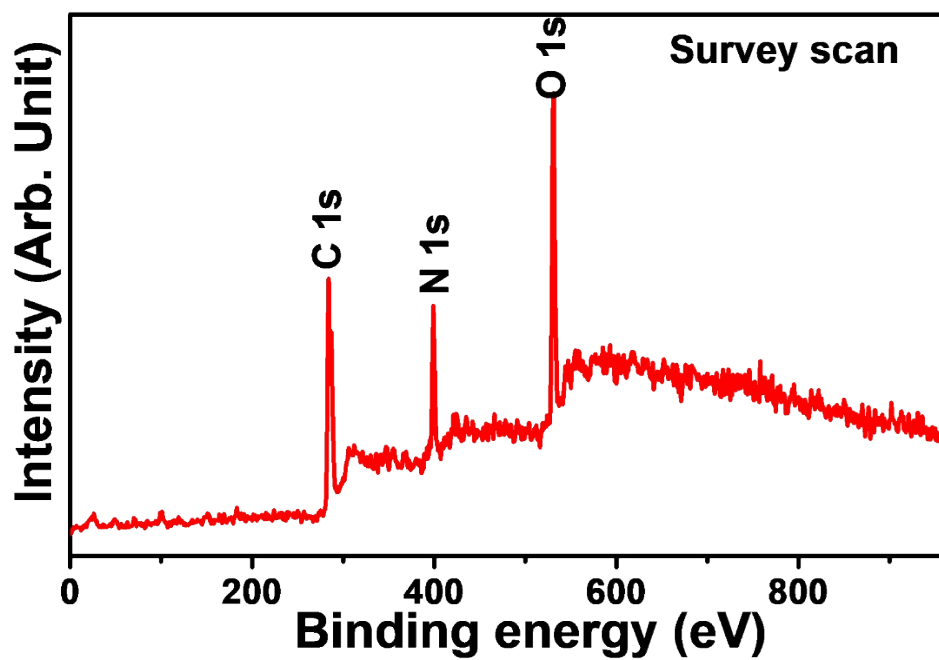


Figure S6: XPS Survey spectra of synthesized CQDs

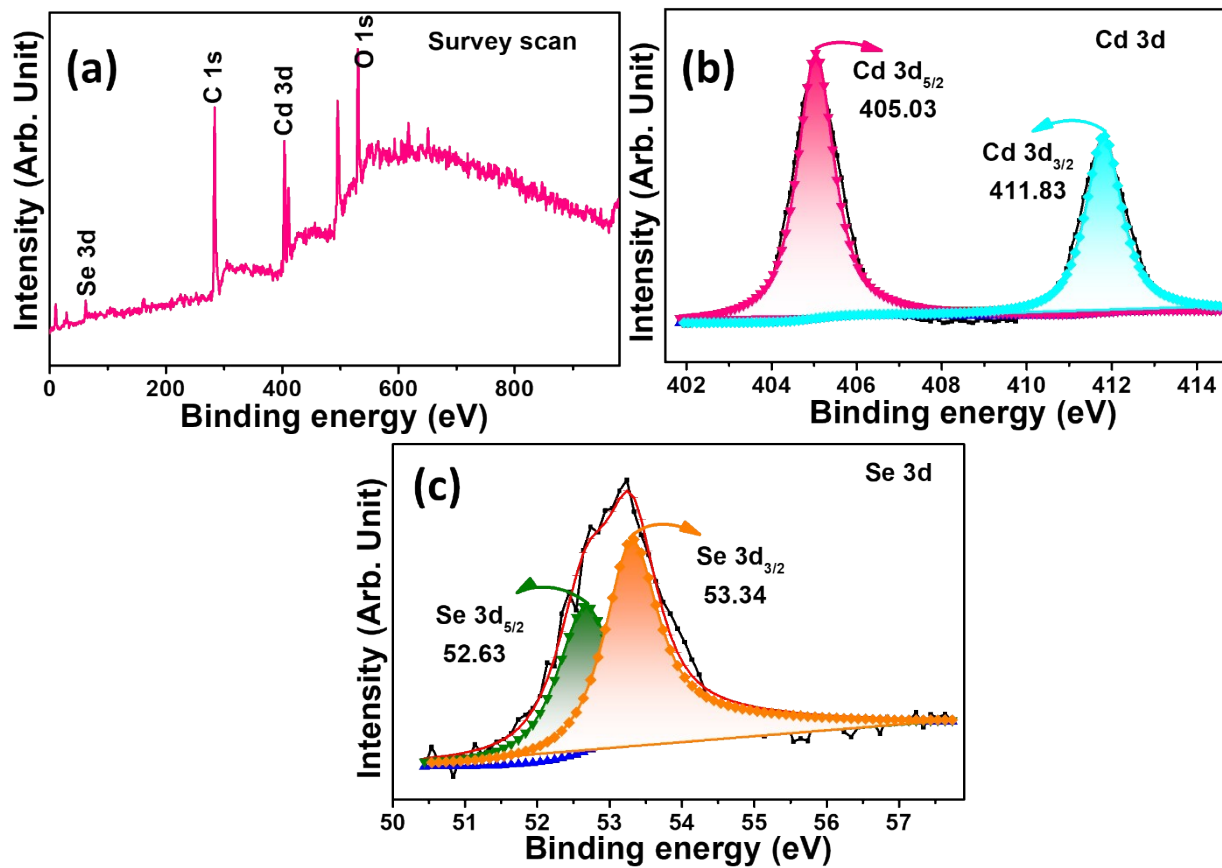


Figure S7: (a) XPS Survey spectra, (b) Cd 3d, (c) Se 3d of synthesized CdSe

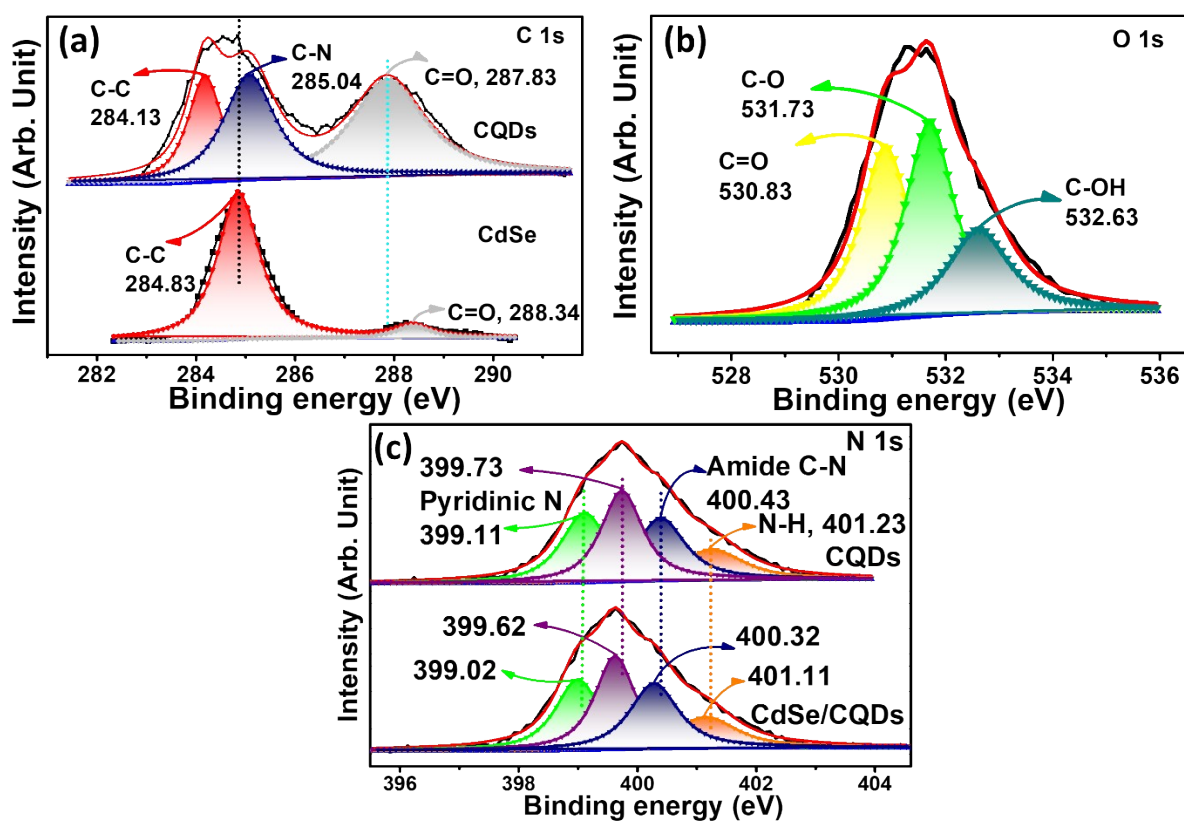


Figure S8: (a) C 1s spectra of synthesized CQDs and CdSe, (b) O 1s spectra of synthesized CQDs, (c) deconvoluted N 1s spectra of CQDs and CQDs/CdSe

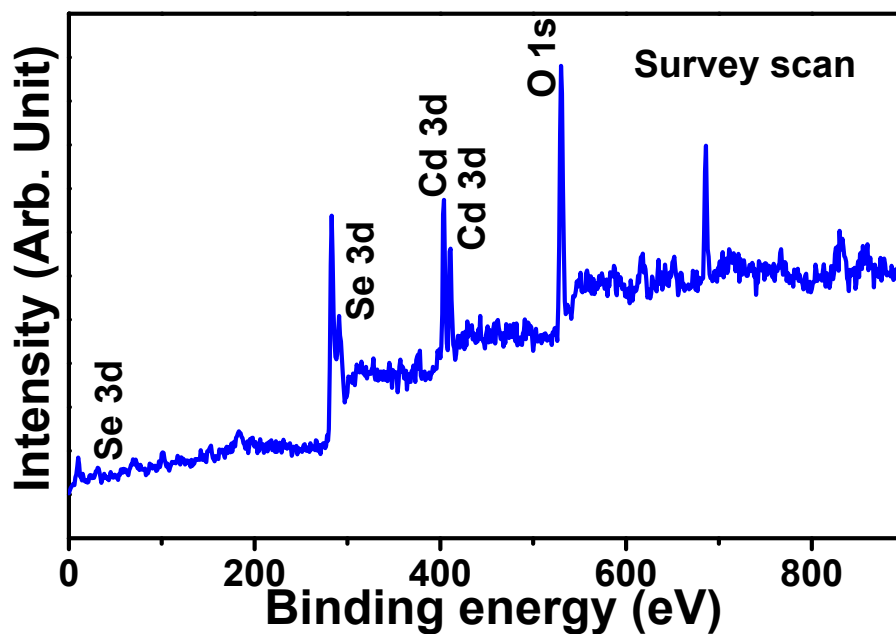


Figure S9: XPS Survey spectra of synthesized CQDs/CdSe (after electrolysis)

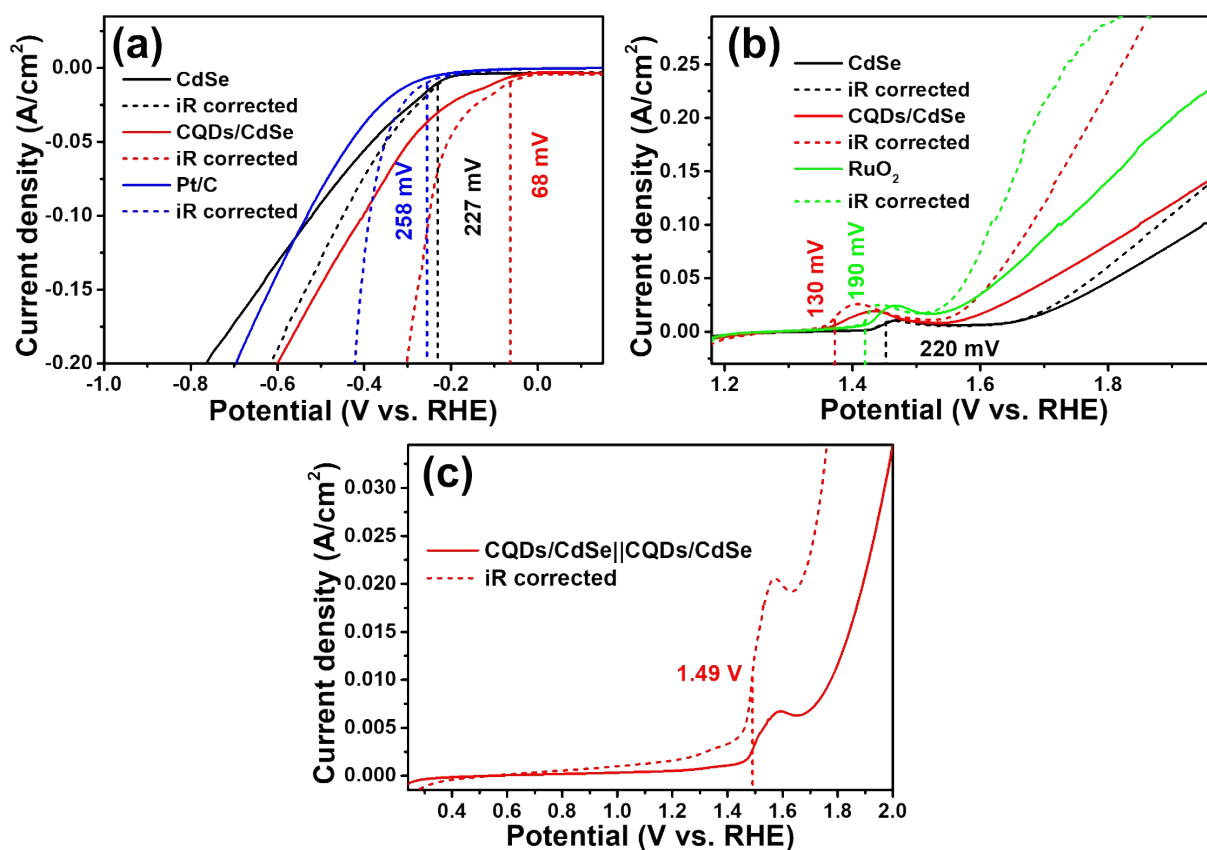


Figure S10: iR corrected linear sweep voltametric curve of CQDs/CdSe, CdSe, Pt/C, RuO₂ for (a) HER, (b) OER and CQDs/CdSe for (c) OWS at a scan rate of 10 mA/cm²

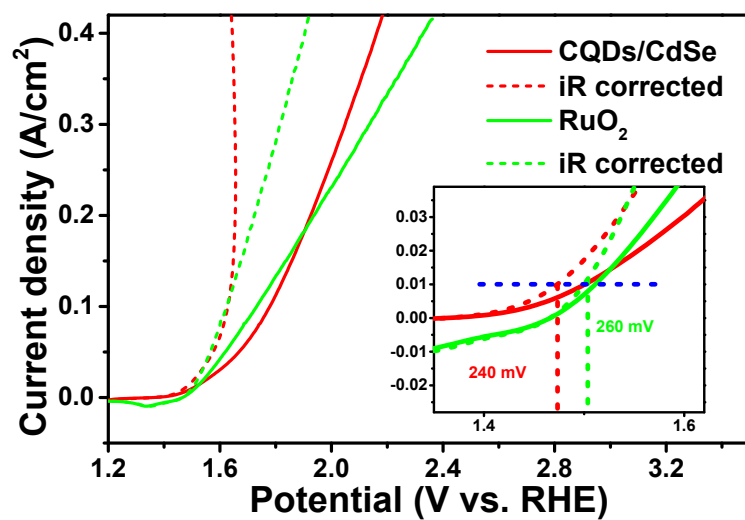


Figure S11: Negative Linear sweep voltametric curve for CQDs/CdSe and benchmark catalyst RuO₂ (inset: overpotential at 10 mA/cm²) performed at 10 mV/s in 1 M KOH.

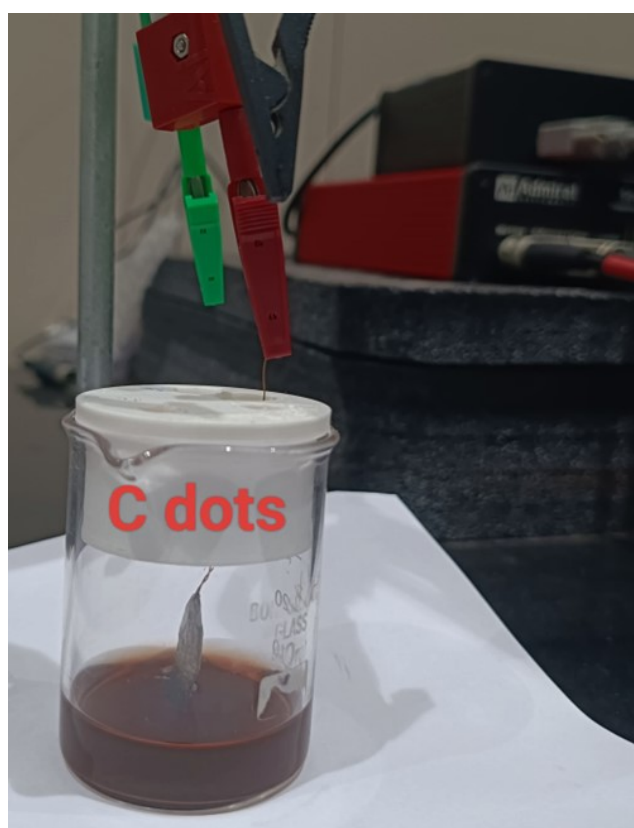


Figure S12: Digital image of performed EC of CQDs

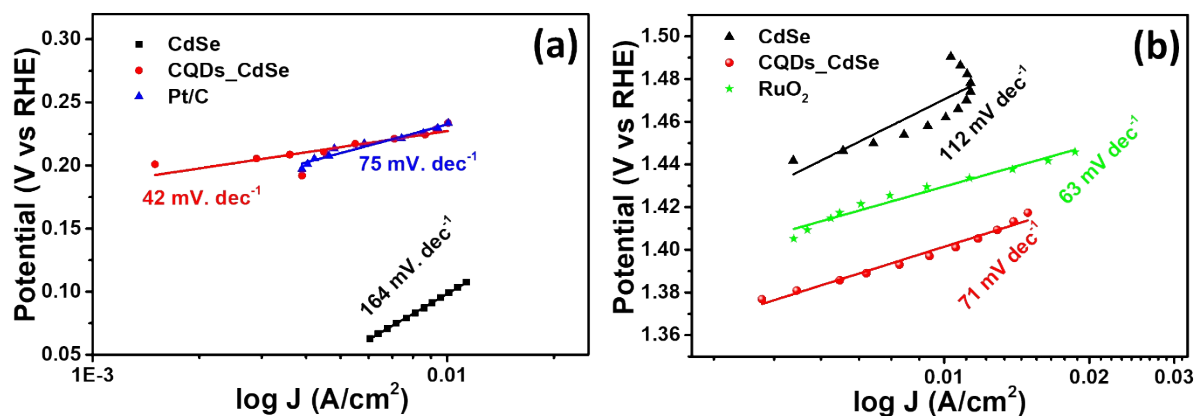


Figure S13: Tafel Slope of (a) HER, and (b) OER where the nanocomposite exhibited a lower tafel slope which indicates the quicker kinetics.

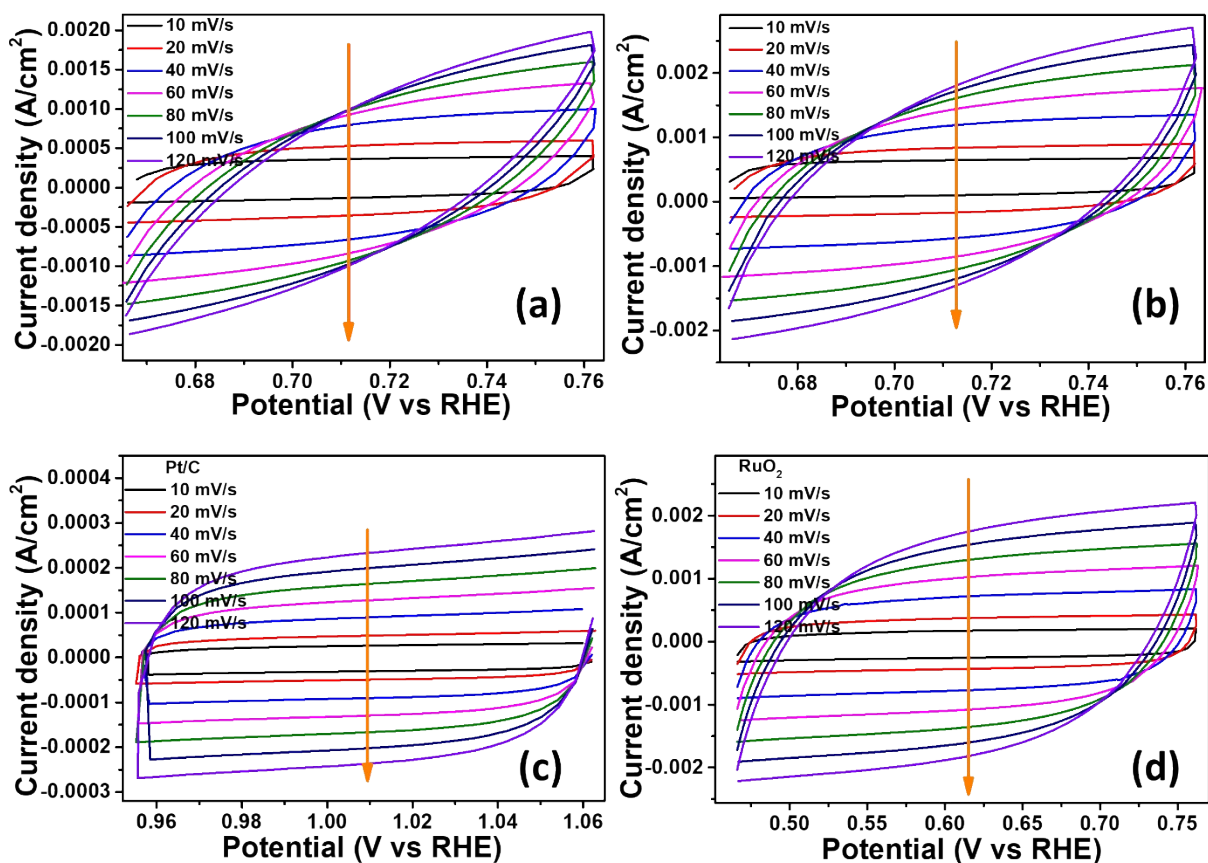


Figure S14: CV cycles in non-faradaic region at different scan rate of (a) CdSe, (b) CQDs/CdSe, (c) Pt/C, (d) RuO₂

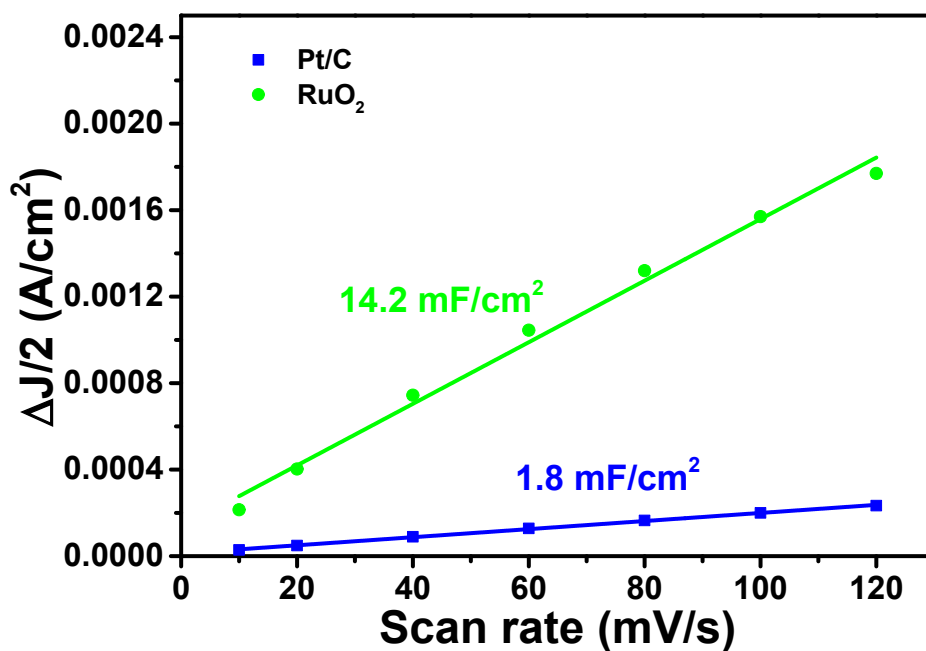


Figure S15: Double layer capacitance (C_{dl}) of Pt/C and RuO_s for the evaluation of electrochemically active surface area (ECSA)

Table S4: Comparison table of the ECSA value of synthesized nanocomposite with the benchmark catalysts

Material	C_{dl} (mF/cm ²)	ECSA (cm ²)
Pt/C	1.8	45
CdSe	6.1	152.5
RuO ₂	14.2	355
CQDs/CdSe	11.1	277.5

Table S5: Comparison table of the synthesized nanocomposite with the reported literatures

Materials	Overpotential (mV)		Tafel slope (mV/dec)		Stability	Reference
	HER	OER	HER	OER		

Co/GQDs	-	330	-	-	60 s	1
NiSe ₂ @NC	220	-	70.6	-	12 h at 20 mA/cm ²	2
CMS - 12 h	190	-	143	-	12 h at 20 mA/cm ²	3
CoSe ₂ @CdSe & CdSe @ CoSe ₂	147 & 110	329 & 140	-	-	-	4
CuO @ CQDs	155	322	-	-	12 h	5
CoNi ₂ S ₄ @CoS ₂ /NF	173	259	-	-	-	6
CQDs/CdSe	99	170	42	71	50 h	This work

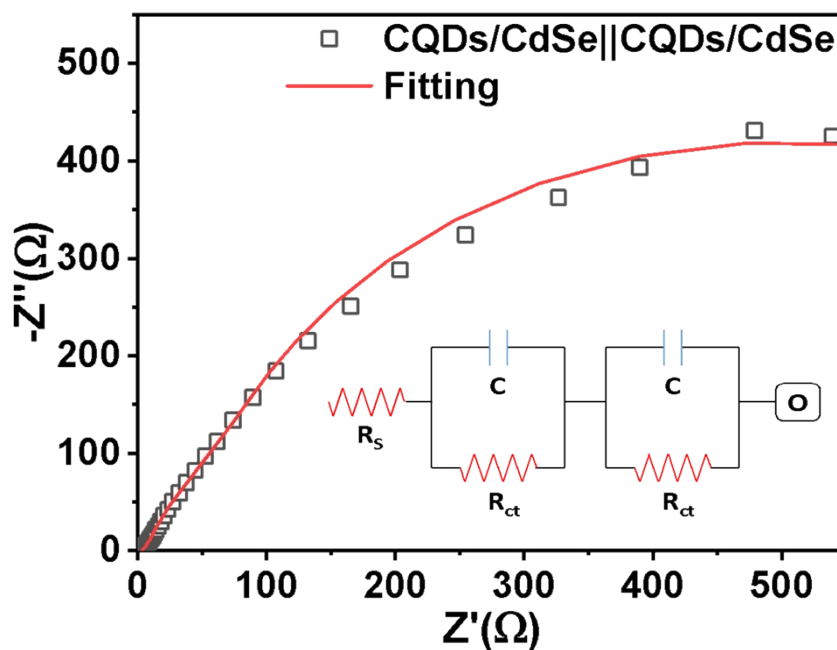


Figure S16: EIS spectra of overall water splitting performed with CQDs_CdSe as anode and cathode in 1 M KOH



Figure S17: Digital image of performed EC on CQDs and CdSe physical mixture as electrode and a visible leaching of material was observed.

Reference

- 1 J. Cirone, S. R. Ahmed, P. C. Wood and A. Chen, Green Synthesis and Electrochemical Study of Cobalt/Graphene Quantum Dots for Efficient Water Splitting, *Journal of Physical Chemistry C*, 2019, **123**, 9183–9191.
- 2 H. H. Do, Q. Van Le, T. H. Lee, S. H. Hong, S. H. Ahn, H. W. Jang and S. Y. Kim, Core-shell architecture of NiSe₂ nanoparticles@nitrogen-doped carbon for hydrogen evolution reaction in acidic and alkaline media, *Int J Energy Res*, 2021, **45**, 20463–20473.
- 3 S. Shit, W. Jang, S. Bolar, N. C. Murmu, H. Koo and T. Kuila, Effect of Ion Diffusion in Cobalt Molybdenum Bimetallic Sulfide toward Electrocatalytic Water Splitting, *ACS Appl Mater Interfaces*, 2019, **11**, 21634–21644.
- 4 K. C. Majhi and M. Yadav, Transition Metal-Based Chalcogenides as Electrocatalysts for Overall Water Splitting, *ACS Engineering Au*, 2023, **3**, 278–284.
- 5 J. S. Kumar, S. Bolar, N. C. Murmu, R. S. Ganesh, H. Inokawa, A. Banerjee and T. Kuila, Synthesis of Tri-functional Core-shell CuO@carbon Quantum Dots@carbon Hollow Nanospheres Heterostructure for Non-enzymatic H₂O₂ Sensing and Overall Water Splitting Applications, *Electroanalysis*, 2019, **31**, 2120–2129.
- 6 R. Huang, W. Chen, Y. Zhang, Z. Huang, H. Dai, Y. Zhou, Y. Wu and X. Lv, Well-designed cobalt-nickel sulfide microspheres with unique peapod-like structure for overall water splitting, *J Colloid Interface Sci*, 2019, **556**, 401–410.

